

# Lawrence Berkeley National Laboratory

## LBL Publications

### **Title**

Understanding performance degradation of Li-cathode

### **Permalink**

<https://escholarship.org/uc/item/0pq3f7g3>

### **Author**

Kim, Haegyum

### **Publication Date**

2025-04-03

Peer reviewed

# Cooperative Research and Development Agreement (CRADA) Final Report

**Report Date: April 3<sup>rd</sup>, 2025**

*In accordance with Requirements set forth in the terms of the CRADA, this document is the CRADA Final Report, including a list of Subject Inventions. It is to be forwarded to the DOE Office of Scientific and Technical Information upon completion or termination of the CRADA, as part of the commitment to the public to demonstrate results of federally funded research.*

**Parties to the Agreement:** Rivian Automotive, LLC and Lawrence Berkeley National Laboratory

**CRADA number:** AWD00006079

**CRADA Title:** Understanding performance degradation of Li-cathode materials (MS Kim Rivian CRADA)

**Responsible Technical Contact at Berkeley Lab:** Haegyum Kim

**Name and Email Address of POC at Partner Company(ies):** Soo Kim, sookim@rivian.com

**Sponsoring DOE Program Office(s):**  
*Office of Vehicle Technologies*

**LBNL Report Number:**  
*LBNL-2001662*

**OSTI Number:**  
*[SPO to complete]*

**Joint Work Statement Funding Table showing DOE funding commitment:**

DOE Funding to LBNL	-
Participant Funding to LBNL	\$195,000
Participant In-Kind Contribution Value	\$300,000
Total of all Contributions	\$495,000

**Provide a list of publications, conference papers, or other public releases of results, developed under this CRADA:**

*None*

**Provide a detailed list of all subject inventions, to include patent applications, copyrights, and trademarks:**

*None*

**Executive Summary of CRADA Work:**

The rapid growth of the electric vehicle (EV) industry has sparked extensive research and development efforts to enhance the performance and efficiency of batteries for EVs. Among the critical components of these batteries, cathodes, i.e., positive electrodes, play a crucial role in determining their overall performance and energy storage capabilities. The physical properties of cathode materials for high-performance battery systems, including elemental composition, particle size, shape, surface coating layer, surface chemical state, and inherent electrochemical properties, are crucial to their overall performance. Process parameters influence these properties and play a vital role in developing efficient battery systems for EVs. Material characterizations, therefore, are of utmost importance in advancing the performance and reliability of EV batteries.

As a part of this project, Rivian Automotive, LLC (hereafter, Rivian) collaborated with Lawrence Berkeley National Laboratory (LBNL) to investigate the relationship between the physical properties and electrochemical performance of various cathode materials, namely  $\text{LiFePO}_4$  (LFP), Mn-substituted LFP ( $\text{LiMn}_x\text{Fe}_{1-x}\text{PO}_4$ , LMFP),  $\text{LiNi}_x\text{Mn}_y\text{Co}_z\text{O}_2$  (NMC), and Al-substituted NMC ( $\text{LiNi}_x\text{Mn}_y\text{Co}_z\text{Al}_p\text{O}_2$ , NMCA). The objective of this partnership was to identify the material characteristics (e.g., structure, chemical, electrochemical, and thermal) that are significant for improving the performance of secondary rechargeable batteries. This is crucial to understand the correlation between material properties and the actual electrochemical performance, emphasizing its significance in this field of research. Rivian screened and provided cathode material candidates. LBNL constructed a material properties database through extensive nano-to-bulk characterizations (SEM, EDX, FIB, TEM, XPS, and XRD) of more than 21 different cathode materials (See Table 1). All the acquired characteristics of materials were analyzed and delivered in a regular biweekly meeting.

Further optimization of electrode coating using different slurry mixing equipment for some LFP cathodes was also carried out. Rivian and LBNL conducted comprehensive electrochemical tests on the representative cathodes, elucidating the relationship between material properties and electrochemical characteristics. As a result, this project has provided valuable

insights into the design and development of high-performance batteries for EVs.

**<Table 1.** List of samples performed nano-to-bulk characterizations under this project >

#	Code	Material	Description	Characterization	
				Rivian	LBNL
1	C007	LFP	Narrow size distribution	XRD, SEM, TD, PD, BET, Raman, XAS	TEM, EDX, TGA, XPS, XAS
2	C014	LFP	Broad distribution	XRD, SEM, TD, PD, BET, Raman, XAS	TEM, EDX, TGA, XPS
3	C039	LFP	Bimodal (S, XL)	XRD, SEM, TD, PD, BET, Raman, XAS	TEM, EDX, TGA, XPS
4	C114	LFP	Small and Medium size	PD	TEM, SEM, EDX, XRD, XPS
5	C115	LFP	Bimodal (S, XL)	PD	TEM, SEM, EDX, XRD, XPS
6	C113	LFP	EV-type	Pd	TEM, SEM, EDX, XRD, XPS, TGA
7	C031	LFP	Bi-modal (S, M)	XRD, SEM, TD, PD, BET, Raman	TEM, EDX, XPS, TGA
8	C011	LFP	Small	XRD, SEM, TD, PD, Raman	TEM, EDX, XPS, TGA
9	C043	LFP	Power-type	PD	TEM, SEM, EDX, XRD, XPS, TGA, Raman
10	C045	LMFP	Mn:Fe (75:25)	XRD, SEM, TD, PD	TEM, XPS, TGA, XAS
11	C080	LMFP	Mn:Fe (60:40)	TD, PD	TEM, SEM, EDX, XRD, XPS, XAS
12	C099	LMFP	Mn:Fe (60:40)	TD, PD	TEM, SEM, EDX, XRD, XPS, XAS
13	C105	LMFP	Mn:Fe (70:30)	TD, PD	TEM, SEM, EDX, XRD, XPS, XAS
14	C120	LMFP	Mn:Fe (60:40)	TD, PD	SEM, EDX, XRD, XPS
15	C052	NMCA	high-Ni NMCA	N/A	SEM, EDX, XRD, XPS, XAS
16	C056	NMC	high-Ni NMC	N/A	SEM, EDX, XRD, XPS, XAS, Coin
17	C050	NMC	high-Ni NMC	N/A	SEM, EDX, XRD, XPS, XAS, Coin
18	C046	NMC	OLO	PD	SEM, EDX, XRD, XPS, XAS
19	C047	NMC	OLO	N/A	SEM, EDX, XRD, XPS, XAS
20	C053	NMCA	NMCA	N/A	SEM, EDX, XRD, XPS
2	C10	NMC	OLO	PD	SEM, EDX, XRD, XPS

1	3				
---	---	--	--	--	--

## Summary of Research Results:

Among the extensive results of characterization, here we show the representative results on each cathode group.

### 1. Powder X-ray diffraction of LMFPs

Mn substitution in Fe-site in LMFP is one of the promising strategies to increase energy density of LFP. This could make electric vehicles more practical, affordable, and appealing to consumers. However, the Mn substitution can also affect the anti-site (Fe/Li or Mn/Li) formation, which is a key parameter determining rate capability. This is why structural analyses are essential to maximize the performance of LMFP. In this project, we measured powder X-ray diffraction in the synchrotron X-ray beamline for accurate evaluation. Our measurement gives up to eight times higher signal-to-noise ratio than the typical Cu-K $\alpha$  radiation in commercial XRD devices; thus, highly precise refinements on structural simulation are achieved.

**Figure 1** shows the structural analysis results of the representative LMFP samples. Interestingly, we found that the correlations in three physical descriptors: Cell volume, anti-site occupancy ratio between Li/transition metal (TM), and Mn content in TM site. The observed positive correlation between the cell volume vs. Mn contents agrees well with the previous studies. Interestingly, we found higher Mn content increases the anti-site occupancy between Li and TM sites (i.e., Mn and Fe).

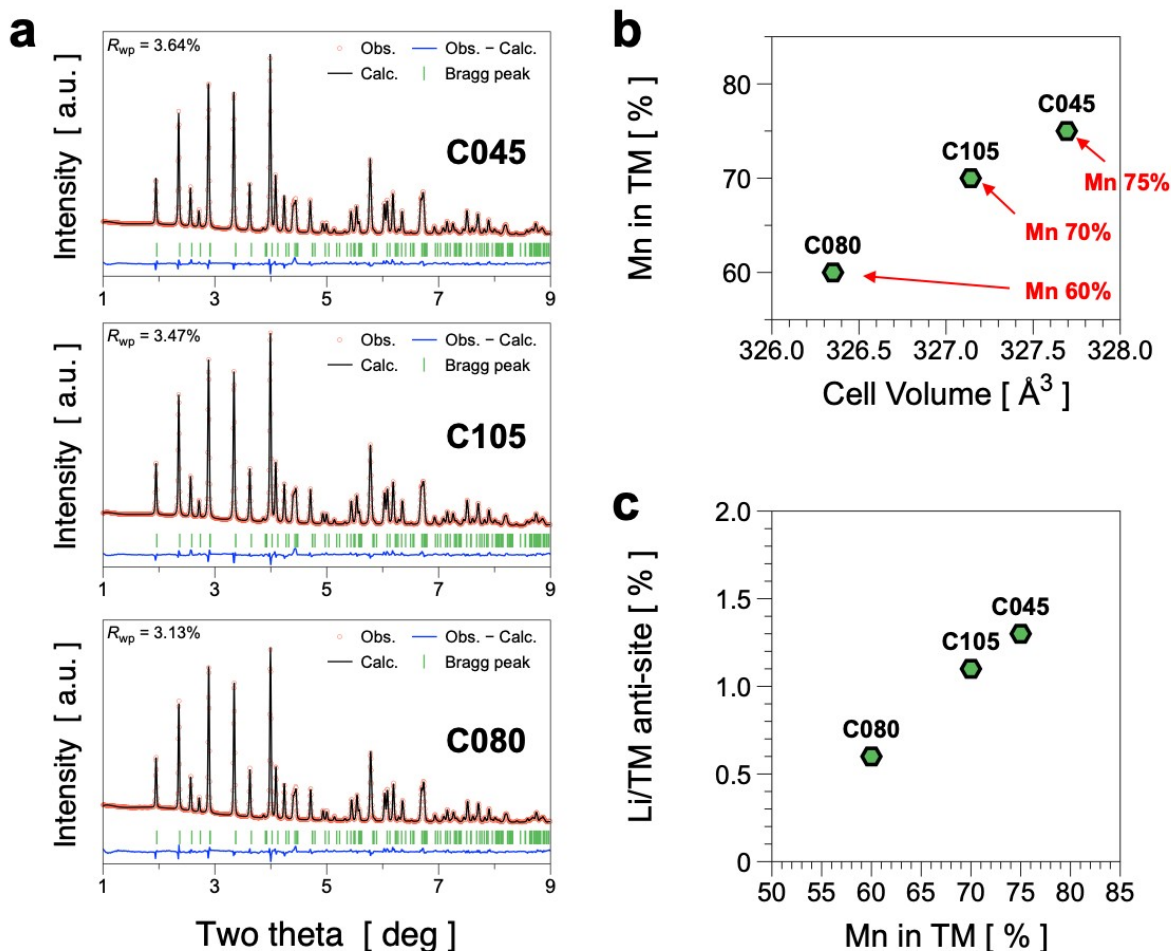


**Figure 1.** (a) Powder X-ray diffraction patterns of the representative LMFPs. Correlation between two obtained physical descriptors. (b) Mn ratio in TM site vs. Cell volume and (c) Li/TM anti-site occupancy vs. Mn ratio. Note that “acceptable” positive correlations are found in the given descriptors: Cell Volume, Mn ratio in TM site, and Li/TM anti-site occupancy.

## 2. HRTEM analysis on the carbon coating layer of LFPs

LiFePO<sub>4</sub> (LFP), with superior stability, longevity, cost-effectiveness, and energy efficiency, is increasingly favored for EVs. The carbon coating on LFP cathodes, which enhances the inherently low electronic conductivity of LFP, is crucial for battery performance. The coating's quality and uniformity significantly affect an LFP-based battery's charge/discharge rates and overall stability. Our study utilized high-resolution transition electron microscopy (HRTEM) to scrutinize the surface carbon coating layer (see **Figure 2**). We implemented a statistical approach, examining over five regions on each particle surface. C007

displayed a narrow distribution compared to C039 and C113. Notably, C039 presented a bimodal size distribution (small and extra-large). Those agree well with the powder size distribution (PSD) analysis results. Intriguingly, irrespective of the particle size, C039 exhibited an uneven carbon coating layer on its surface.

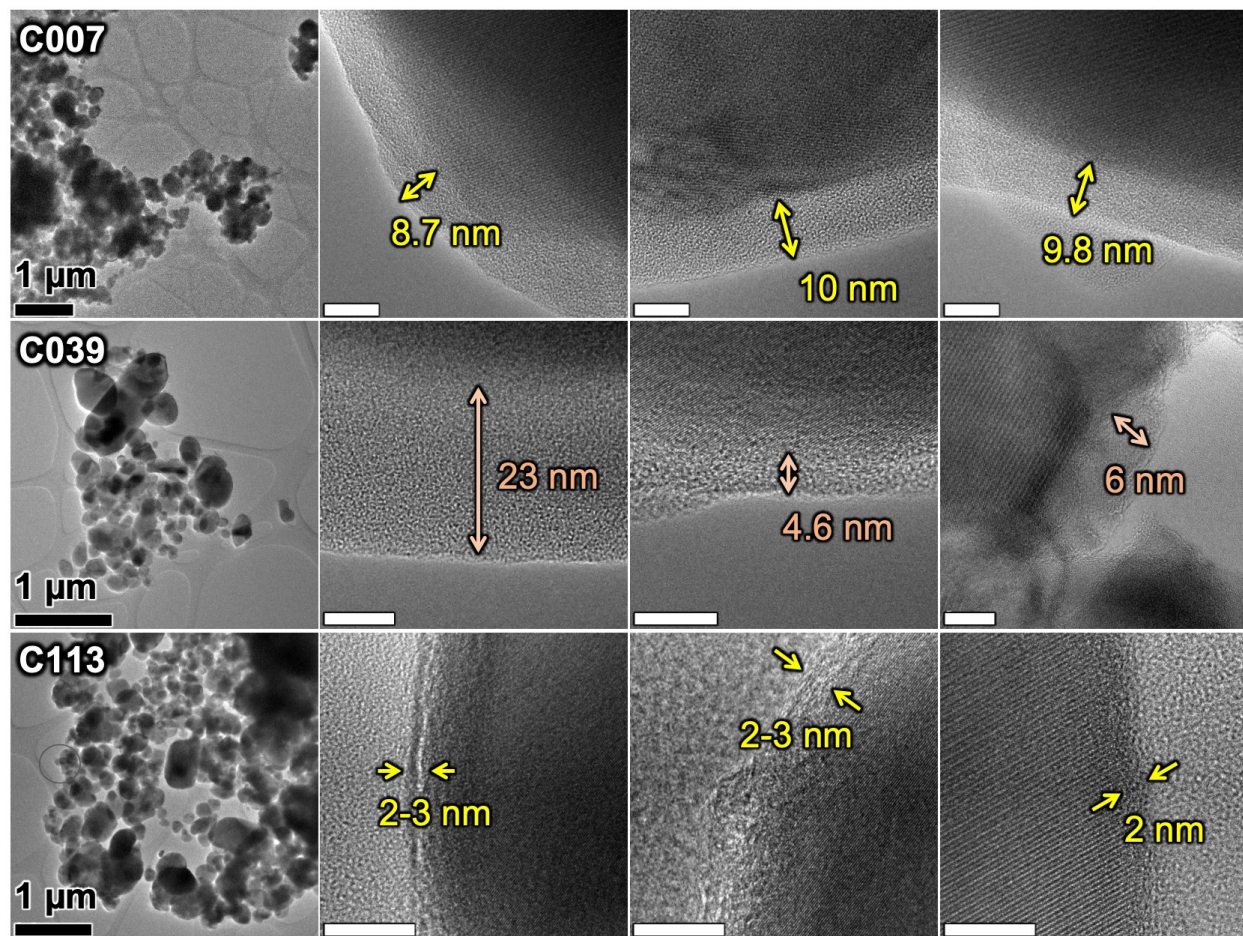


**Figure 2.** normal and high-resolution TEM images acquired from representative LFP samples: (top) C007, (middle) C039, and (bottom) C113. Note that the white scale bars are 10 nm.

### 3. SEM-EDX for single crystalline (SC) and polycrystalline (PC) NMC particles

NMC cathodes have been extensively investigated as one of the most promising materials for next-generation high-energy Li-ion batteries for EVs. Single crystalline particles have enhanced structural strength and tap density and are highly robust against microcracking. NMC usually adopts a conventional morphology of secondary structure that combines numerous

nano-sized primary particles aggregate together to form a larger particle. These polycrystalline particles have the unique advantages of not only shortening the Li-ion diffusion pathway but also improving its power. The morphology of SC/PC NMC particles and SC NMC particles are shown in **Figure 3**. SC/PC NMC particles (**Figure 3a**) comprise bimodal primary particles of <500 nm and 2  $\mu\text{m}$  that comprise the spherical secondary particles. EDX elemental mapping (**Figure 3b**) displayed uniform manganese, nickel, cobalt, and oxygen distribution on the particle surface. In contrast, the SC NMC (**Figure 3c**) exhibited 1-2  $\mu\text{m}$  particles where some particles were agglomerated. In this case, EDX elemental mapping (**Figure 3d**) demonstrated a uniform distribution of manganese, nickel, cobalt, and oxygen over the particles.

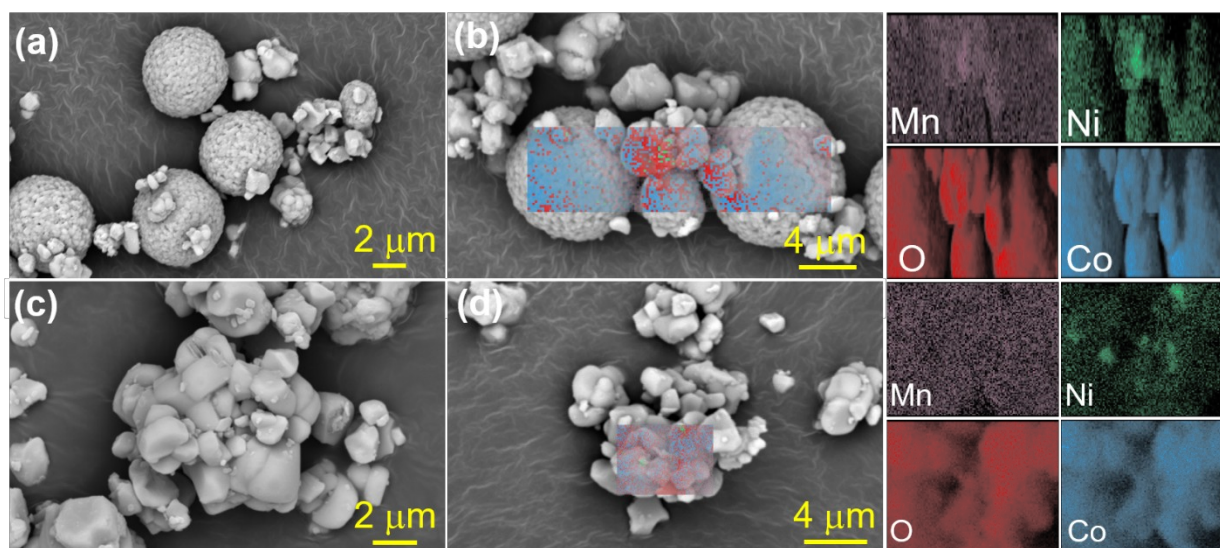


**Figure 3.** (a) SEM image and (b) corresponding EDX elemental mapping of single crystalline and polycrystalline NMC. (c) SEM image and (d) corresponding EDX elemental mapping of single crystalline NMC.

#### 4. Electrochemical test on LFPs

The electrochemical performance of LFP cathodes was tested in a half-cell configuration. LFP electrodes were prepared by mixing 80% active material with 10% super C65 and 10% polytetrafluoroethylene (PTFE) binder and subjected to galvanostatic cycling (**Figure 4**) at low current rates (0.1 C) in voltage range 2.8-4.0 V. At a low current density of 0.1C, LFP cathodes (C018) with primary and secondary particles exhibited stable cycling with capacity retention of 99% after 100 cycles compared to LFP cathodes with different particle distribution. Further, galvanostatic charge-discharge profiles of C018

demonstrated a flat charge and discharge plateaus with a high initial discharge capacity of 156 mAh g<sup>-1</sup> at 0.1C. Interestingly, C039 showed the worst cyclic stability among the samples. We suspect that's because of its unevenly carbon coated layer, as shown in **Figure 2**.

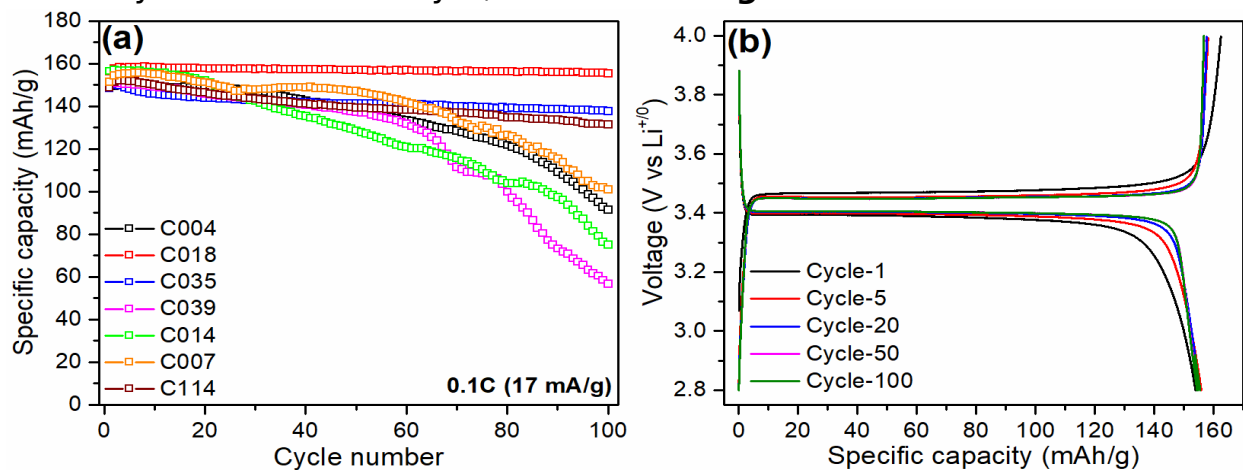


**Figure 4.** (a) Galvanostatic cycling of LFP cathodes at a current density of 0.1C (17 mA g<sup>-1</sup>). (b) Galvanostatic charge-discharge profiles of C018 LFP cathode at current density of 0.1C in the voltage range 2.8-4.0 V